



ELSEVIER

Contents lists available at ScienceDirect

## Comptes Rendus Physique

www.sciencedirect.com



Ultra-high-energy cosmic rays / Rayons cosmiques de ultra-haute énergie

## Cosmic rays and hadronic interactions



## Rayons cosmiques et interactions hadroniques

Paolo Lipari

INFN, Roma "La Sapienza", Italy

## ARTICLE INFO

## Keywords:

Cosmic rays  
Hadronic interactions  
Mass composition  
Forward physics

## Mots-clés:

Rayons cosmiques  
Interactions hadroniques  
Composition en masse  
Physique à l'avant

## ABSTRACT

The fields of cosmic rays and hadronic interactions are intimately related. High-energy cosmic rays can only be studied detecting the showers they generate in the atmosphere, and the interpretation of the data requires the precise modeling of hadronic interactions. Uncertainties in this modeling are in many cases an important limitation for cosmic ray studies. The cosmic ray spectrum extends to particles with energy  $E \sim 10^{20}$  eV, which, assuming that the primary particle is a proton, corresponds to a nucleon–nucleon c.m. energy  $\sqrt{s} \simeq 430$  TeV, 50 times higher than the current LHC energy. Cosmic ray studies require an extrapolation of the results obtained at accelerators, but also offer the possibility to perform studies on the properties of hadronic interactions that are impossible at accelerators.

© 2014 Published by Elsevier Masson SAS on behalf of Académie des sciences.

## R É S U M É

Les domaines d'études des rayons cosmiques et des interactions hadroniques sont intimement liés. Les rayons cosmiques d'ultra haute énergie ne peuvent être étudiés qu'à travers les cascades qu'ils génèrent dans l'atmosphère. L'interprétation de ces données demande une modélisation précise des interactions hadroniques. Les incertitudes dans ces modélisations limitent ainsi bien souvent ces études. Le spectre des rayons cosmiques s'étend jusqu'à des énergies  $E \sim 10^{20}$  eV, ce qui, en supposant que la particule primaire est un proton, correspond à une énergie centre de masse  $\sqrt{s}$  d'environ 430 TeV, soit 50 fois plus élevée que celle disponible en 2013 au LHC. L'étude des rayons cosmiques demande donc une extrapolation des résultats obtenus auprès des accélérateurs, mais offre aussi la possibilité d'étudier les interactions hadroniques à des énergies inaccessibles auprès de ces machines.

© 2014 Published by Elsevier Masson SAS on behalf of Académie des sciences.

## 1. Introduction

The flux of very-high-energy cosmic rays is so small that it is impossible to place above the atmosphere instruments with an acceptance sufficiently large to detect directly the primary particles. Cosmic rays (CR) can only be studied via the

E-mail address: [paolo.lipari@email.roma1.infn.it](mailto:paolo.lipari@email.roma1.infn.it).

observation of the showers they generate in the atmosphere, and to reconstruct their energy spectrum and composition, it is necessary to have a sufficiently good understanding of the development of hadronic showers in the air. Uncertainties in the description of the properties of hadronic interaction are, at least in principle, the main difficulty in performing this program.

There are very strong arguments to believe that the underlying theory that describes the interactions between hadronic particles is Quantum Chromo Dynamics (QCD). The fundamental fields in the theory are quarks (spin 1/2 fermions) and gluons (massless spin 1 gauge bosons), while the physical hadrons are bound states composed of three quarks in the case of baryons (three anti-quarks in the case of anti-baryons), or a quark and anti-quark in the case of mesons. QCD is an asymptotically free theory in the limit where the fundamental fields interact at very short distances (and have scattering with large momentum transfer). For ‘hard’ (large  $Q^2$ ) processes, one can then use perturbation theory to compute cross sections with high accuracy. On the other hand, the force between colored partons does not decrease with distance, and one has the phenomenon of “confinement”, i.e. quarks and gluons cannot be observed as free objects. A viable method to compute from first principles the cross sections of “soft” (low  $Q^2$ ) processes with reasonable precision is not known. Soft processes account for most of the cross section in hadronic interaction, and therefore the prediction of the development of hadronic showers is a difficult task, which requires bridging the gap between ‘hard’ and ‘soft’ hadronic physics.

The data obtained at accelerators can (in fact have to) be used to determine experimentally many properties of hadronic interaction. A purely phenomenological approach is however not possible, because the data do not cover the entire kinematical space relevant for CR studies, and one needs to extrapolate the experimental results outside the region where they have been obtained. The most interesting extrapolation is for the center of mass energy of the hadron–hadron collisions. The CR spectrum extends (at least) to  $E \simeq 10^{20}$  eV, which corresponds for proton primaries to a c.m. energy for nucleon–nucleon interactions  $\sqrt{s} \simeq 433$  TeV, much higher than the maximum energy obtained at the LHC collider at CERN. In the development of CR showers also the interactions of mesons (especially pions and kaons) play an important role, and in this case the required extrapolation is larger and more uncertain, since the experimental results, obtained in fixed target experiments, extend only to much lower energy ( $\sqrt{s} \simeq 27$  GeV or  $E_{\text{lab}} \simeq 400$  GeV).

Extrapolations are also needed in the kinematical space of secondary particles. The particles in the final state of an interaction that play the most important role in the development of CR showers are those that carry a large fraction of the projectile particle energy. These particles transport energy deeper in the atmosphere, and their spectra and properties must be accurately described. The so-called “projectile fragmentation region” is however the kinematical region where the measurements in collider experiments are most difficult, because the particles have very small angles with respect to the accelerator beams. In the absence of direct measurements, one can only rely on extrapolations of the results obtained for lower-energy particles. Efforts to study experimentally the very forward region at LHC experiments are therefore very important.

One should of course also remember that CR showers develop in the air, where the targets are nuclei (nitrogen, oxygen, and argon), and that a significant part of the CR are nuclei. The interpretation of CR observations requires then the modeling of hadron–nucleus and nucleus–nucleus interactions, while much of the data available at the highest energies have been obtained in hadron–hadron collisions. For example, we now have measurements of the  $pp$  total and elastic cross section up to  $\sqrt{s} = 8$  TeV, but the proton–nucleus and nucleus–nucleus cross sections at the same c.m. energy can only be calculated (using extensions of the Glauber theory), introducing theoretical uncertainties. For this reason, the experimental programs for proton–nucleus and nucleus–nucleus collisions at RHIC and LHC have been, and will be of great interest for the CR community.

The relation between cosmic rays and hadronic physics can be rich and complex. The results of accelerators experiments on hadronic collisions (and the theoretical frameworks constructed for their interpretation) are used to understand the nature of the CR fluxes, but the results of CR observations can also be used to obtain information on hadronic interactions in regions of kinematical space that are not accessible with accelerators. This task can appear impossible, because the properties of the CR beam are not known a priori, and have to be determined experimentally from the same observations as those used to study hadronic interactions. However, the requirement of a consistent interpretation for a well-chosen set of observations can in principle break the apparent circularity of the problem.

## 2. Hadronic interactions

In QCD protons and neutrons are complicated, spatially extended objects formed by many elementary objects. The “valence” content of a proton is two up (electric charge +2/3) quarks and one down (charge –1/3) quark, but at a deeper level one finds in the proton a very large (in fact diverging) number of partons, since quarks can radiate gluons, and the gluons can create  $q\bar{q}$  pairs. The Parton Distribution Functions (PDF’s)  $F_j(x, Q^2)$  describe the probability of finding a parton of type  $j$  with a fraction  $x$  of the proton momentum (in a frame where the  $p$  has a very large energy) when probing at the scale  $Q^2$ . The  $Q^2$  evolution of the PDF’s is calculable in QCD, but only starting from an initial condition that is determined experimentally. Convoluting the PDF’s with cross section it is then possible to compute with high accuracy cross sections for hard processes (such as the production of a high  $p_{\perp}$  jet–pair, or a Higgs boson), on the other hand a hadron collision can be seen at a fundamental level as resulting in many parton–parton interactions, most of which are soft and poorly understood.

The spatial extension of the nucleons can be studied in electron scattering experiments. The proton electromagnetic form factor is well described by the expression  $F(Q^2) \simeq [1 + r_0^2 Q^2]^{-2}$  with  $r_0 \simeq 0.234$  fm. This corresponds (after performing a

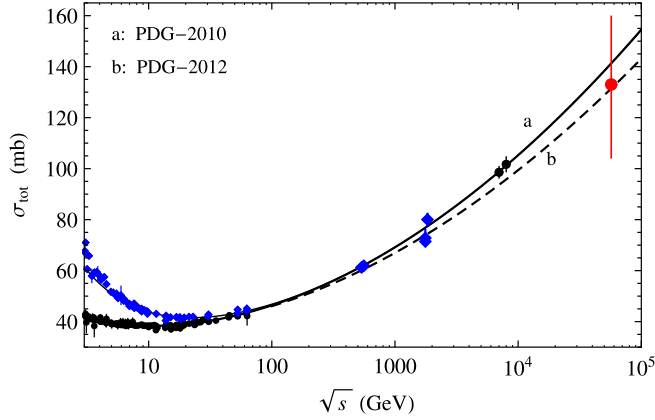


**Fig. 1.** Total  $pp$  and  $\bar{p}p$  cross section. The lines are the predictions of PDG–2010 [1] and PDG–2012 [2]. The point at  $\sqrt{s} = 57$  TeV was estimated by the Auger Collaboration from CR observations [29].

Fourier transform) to an electric charge density distribution that is approximately exponential ( $\rho(r) \propto e^{-r/r_0}$ ). Electron (and neutrino) scattering at larger  $Q^2$  (smaller distances) reveals how the electric charge is associated with point-like partons (the quarks). The order of magnitude of the  $pp$  hadronic cross section is in fact determined by the proton spatial extension ( $\sigma_{pp} \sim \pi(4r_0)^2 \simeq 28$  Mbarn). The  $pp$  cross section grows slowly with c.m. energy as illustrated in Fig. 1, which includes the measurements obtained at LHC by the TOTEM detector for  $\sqrt{s} = 7$  and 8 TeV, and the estimate obtained from CR observations by the Auger Collaboration at  $\sqrt{s} = 57$  TeV (see discussion below). The lines in the figure are functional fits to the  $pp$  cross section from the 2010 [1] and 2012 [2] versions of the Particle Data Group review. In these parameterizations, the cross section grows  $\propto \ln^2 s$ , the same energy dependence of the so-called “Froissart bound”. The question of whether there is a robust theoretical understanding behind this result remains controversial (see, for example, the discussion in [3]).

The growth with energy of  $\sigma_{\text{tot}}(s)$  can be interpreted qualitatively as the consequence of the fact that the number of parton–parton interactions increases when the kinematical space expands. This idea implies that the growth of the cross sections should also be accompanied by a more complex structure of the final states due to the presence of multiple parton interactions in the same collision.

In essentially all existing models, multiple interactions in hadron collisions are included in the theoretical framework using an eikonal formalism. The elastic scattering amplitude (which gives also the total cross section via the optical theorem) is written as an integral in impact parameter space:

$$f_{\text{el}}(q, s) = i \int \frac{d^2b}{2\pi} e^{i\vec{q}\cdot\vec{b}} \Gamma(b, s) = i \int \frac{d^2b}{2\pi} (1 - e^{i\chi(b, s)}) \quad (1)$$

where  $\vec{q}$  is the transfer momentum (approximated as a purely transverse spatial vector),  $\Gamma(b, s)$  is the profile function, and  $\chi(b, s)$  the eikonal function.

The theory attempts to connect the eikonal function to the parton–parton cross section. In the simplest models one writes:

$$\chi(b, s) \simeq \frac{1}{2} \sigma_{\text{parton}}(s) A(b, s) \quad (2)$$

$\sigma_{\text{parton}}(s)$  is the total cross section for parton interactions (that has contributions from both hard and soft interactions) and  $A(b, s)$  is a profile function that describes the overlap of the spatial (impact parameter space) distributions of hadronic matter in the colliding protons. Note that Eq. (2) implies that the ratio  $\sigma_{\text{parton}}(s)/\sigma_{\text{inel}}(s)$  gives the average number of elementary interactions per inelastic collision.

A discussion of the problems associated with the definition of a parton cross section, and the meaning of an elementary soft interaction is beyond the scope of this brief review. Many questions remain very controversial in what is sometimes called “Gribov–Regge multiple scattering theory” [4]. Also very controversial from the theory point of view is the role of the pomeron (or pomerons) in hadronic physics, which for some is an important theoretical object, and for other is a misleading, ill-defined or perhaps even meaningless concept (for a discussion, see [5]).

The structure of the final state of inelastic hadron interactions (particle composition, multiplicity, energy spectra, fluctuations and so on) is of great importance for shower development. If the particles in the final state have on average large (small) energy, the showers are more (less) penetrating. For this reason it is important to describe correctly the relative importance of the diffractive and non-diffractive components in the inelastic cross sections that accounts for approximately 20% (80%) of the inelastic cross sections. Diffractive interactions can be seen as processes where one (or both) of the colliding protons is (are) excited into a state with the same internal quantum numbers as the initial particle; the beam and projectile particles then undergo an elastic scattering with small momentum transfer. Accordingly, the diffractive cross

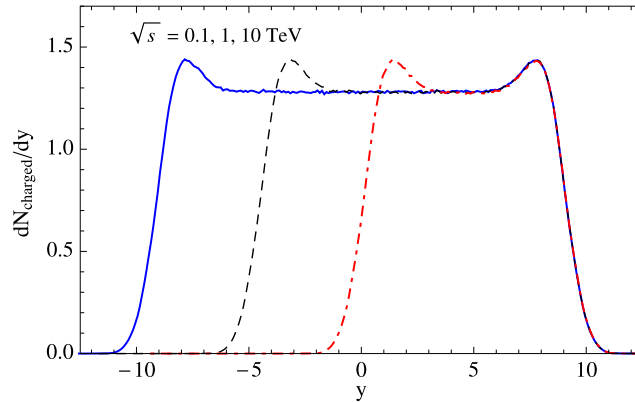


**Fig. 2.** Example of the rapidity distributions of particles obtained from the fragmentation of a  $u\bar{u}$  string, calculated with Monte Carlo methods using the LUND algorithm [12] for three values of the mass of the system (0.1, 1 and 10 TeV). The distribution for the highest mass is shown in the c.m. system, in the other cases the distribution is boosted to have the same  $y_{\max}$ .

section can be naturally divided into three components: target, beam and double diffraction. The mass distribution of the excited state peaks at low masses (with the  $\Delta$  resonance with  $m_{\Delta} \simeq 1.232$  GeV playing a prominent role). Single diffraction events in  $pp$  collisions have therefore one proton that carries an energy close to the initial state particle in one hemisphere, and a small number of high energy particles (formed by the decay of the excited nucleon resonance) in the opposite hemisphere. In double diffraction events, the sets of particles produced in the decay of two resonances are separated by a “rapidity gap”.

From the point of view of theory, the problem is to predict the diffractive cross section in a consistent way. This can in principle be obtained in multi-channel eikonal model (see, for example, the discussion in [6,7]).

In non-diffractive events, nearly all the secondary particles are produced with a small transverse momentum (with respect to the direction collinear with the momenta of the initial state particles) and a broad distribution in longitudinal momentum. The  $p_{\perp}$  distribution is approximately Gaussian, with an average of the order of 0.3–0.5 GeV (which depends on particle type and c.m. energy). The  $p_{\perp}$  distribution has a power-law tail that becomes more important with increasing  $\sqrt{s}$ , and can be understood as the result of the increasing importance of hard scattering between partons.

The longitudinal momentum distribution can be best described in the c.m. frame, where most of the secondaries are soft. The inclusive spectra for mesons are strongly suppressed when the longitudinal momentum is close to the kinematical limits ( $p_{z,\max} \simeq \pm\sqrt{s}/2$ ). In the case of nucleons, one finds one “leading” nucleon per hemisphere with large momentum and a distribution that extends to the kinematical limit.

In 1969, Feynman, extrapolating the first observations of the experimental results available at the time, suggested [8] that the inclusive differential energy spectra of the final state particles satisfy asymptotically (at large  $\sqrt{s}$ ) a scaling property, now known as “Feynman scaling”:

$$\frac{dN_j}{dp_z}(p_z, \sqrt{s}) \simeq \frac{1}{E} F_j \left( \frac{2p_z^*}{\sqrt{s}} \right) = \frac{1}{E} F_j(x_F) \quad (3)$$

In the equation above,  $N_j$  is the number of particles of type  $j$  produced in the interaction, and  $dp_z/E$  is a relativistic invariant. The important point is that the function  $F_j$  depends only on the ratio  $x_F = 2p_z^*/\sqrt{s}$  (or ‘x-Feynman’, with  $p_z^*$  the momentum in the c.m. frame) for all values of the c.m. energy  $\sqrt{s}$ . When  $x_F \rightarrow 0$ , the function  $F_j(x_F)$  takes a finite value, and the inclusive spectra become approximately  $dN_j/dp_z \propto 1/E$ . Introducing the rapidity  $y$  defined by the differential equation:  $dy = dp_z/E$ , which can be integrated to obtain (for the boundary condition  $y = 0$  when  $p_z = 0$ )  $y = 1/2 \log[(E + p_z)/(E - p_z)]$ . The  $x_F \rightarrow 0$  limit can be restated, saying that the rapidity distribution  $dN_j/dy$  in the central region ( $y = 0$  in the c.m. frame) is flat, with a constant ( $\sqrt{s}$  independent) value.

Feynman scaling is *not* an exact property of the spectra in the final states of hadron–hadron collisions; however, it is an important concept for hadronic interactions, because it is a property of the hadronization of certain parton systems with identical structure but different mass. For example, a  $q\bar{q}$  system created in  $e^+e^-$  annihilation at  $\sqrt{s} = M$  fragments into a set of hadrons that have spectra that are experimentally consistent with Feynman scaling. The iterative algorithms for the fragmentation of such a  $q\bar{q}$  system developed following the Field and Feynman ansatz [9] are now in common use in different Monte Carlo codes (such as those of the Lund group [10]). An illustration of this scaling behavior is shown in Fig. 2.

Assuming the validity of Feynman scaling, it would be straightforward to extrapolate the existing accelerator data to arbitrary energy predicting shower development for CR of an arbitrary primary energy. On the other hand, the scaling is violated in high-energy hadron collisions. The clearest evidence for the existence of scaling violations is the measurement of the charged particle rapidity distributions for collisions at different  $\sqrt{s}$ . Experimentally, it is in fact simpler to measure the distribution for the variable pseudo-rapidity:  $\eta = 1/2 \ln[(p_z + p_{\perp})/(p_z - p_{\perp})] = 1/2 \ln[(1 + \cos\theta)/(1 - \cos\theta)]$ . The

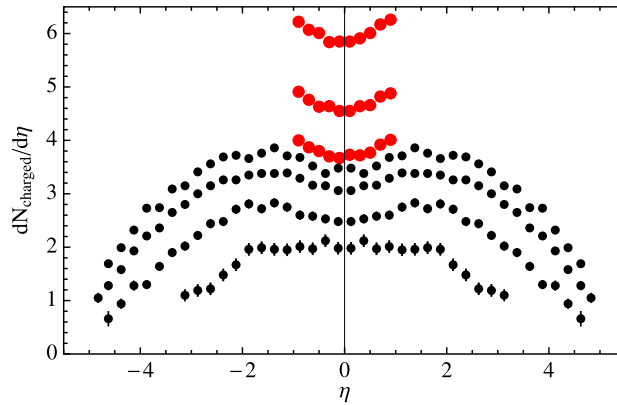


**Fig. 3.** Pseudorapidity distributions measured in  $\bar{p}p$  interactions by the UA5 experiment at the CERN SpS collider at  $\sqrt{s} = 53, 200, 546$  and  $900$  GeV, and in  $pp$  interactions by ALICE at LHC at  $\sqrt{s} = 0.9, 2.36$  and  $7$  TeV.

pseudorapidity  $\eta$  depends only on the (more easily measured) direction of the particle, and is identical to the rapidity  $y$  in the case of massless particles. The particle density  $dN/d\eta$  for  $\eta \simeq 0$  grows with  $\sqrt{s}$ , as shown in Fig. 3 (note that a flat distribution for  $y$  corresponds to an  $\eta$  that has minimum at  $\eta \simeq 0$  because of the Jacobian factor in the variable transformation).

Because of energy conservation, to the increase in the particle density in the central region corresponds a softening of the spectra in the two-fragmentation region, that is a suppression of the production of particles at large  $|x_F|$ . This effect is phenomenologically very important for CR. In fact, looking at the collision in the laboratory frame, particles in the backward hemisphere ( $x_F < 0$ ) have low energy (of the order of  $E_{\text{lab}} \simeq \sqrt{m^2 + p_{\perp}^2}$ ), but for particles in the forward hemisphere ( $x_F > 0$ ), one has  $E_{\text{lab}} \simeq E_0 x_F$  (with  $E_0$  the primary energy), and  $x_F$  distribution can then be simply interpreted as the laboratory energy distribution.

As already discussed, some of the properties of hadronic interactions that are most significant for the development of CR showers, such as the energy distribution of the leading nucleon, and in general of particles at large  $|x_F|$  are very difficult to measure in collider experiments, because particles at very small angles are very difficult to observe. Special detectors such as LHCf have been operating to study the fastest secondary particles in collisions at LHC. The LHCf results [11] show interesting discrepancies with the available Monte Carlo results. The implication of these results for CR shower development are still not clear, because the data were obtained in a very restricted kinematical region, and the determination of the inclusive energy spectra depends on assumptions about the  $p_{\perp}$  distributions. A more complete coverage of  $p_{\perp}$  for high energy secondaries could resolve these ambiguities and would be very beneficial.

Several Monte Carlo models have been constructed for the generation of  $pp$  collisions. Some of these codes such as PYTHIA, HERWIG or SHERPA [13–16] have as primary goal the interpretation of the accelerator collisions, with the main focus on rare hard processes, including manifestations of possible new physics. Also in this case, it is however necessary to address the problem of the properties of particles produced in soft interactions (the so-called “underlying event” in the collisions where a hard process has been identified).

In most cases the codes developed for experiments at accelerators cannot be easily used for CR studies, because they lack the possibility to model the interactions of mesons, or nuclei, or change easily the c.m. energy of the interactions during a single computer run, as required for shower simulations. Because of these limitations, other Monte Carlo models such as QGSJET, SIBYLL or EPOS [17–20] are in common use for the simulations of CR showers.

The models used at accelerators have versions with the parameters “tuned” to be in agreement with the data obtained at a fixed  $\sqrt{s}$ . The codes used for CR studies (that neglect the rare processes of highest interest in particle physics) optimize their parameters to reproduce the data in a very broad range of  $\sqrt{s}$  because showers contain particles of all energies below the energy of the primary. In addition, the codes for CR studies at the highest energies need to consider the extrapolation beyond the range accessible at the colliders. This can be an important constraint in choosing the energy dependence of the model parameters. The Monte Carlo models are reasonably successful in describing the LHC results, but some discrepancies remain, and the robustness of the extrapolations needed for CR studies is still controversial. For more discussion, see [21,22].

### 3. Cosmic ray shower development

A very brief outline of the development of a proton cosmic ray shower can be summarized as follows. The primary particle penetrates in the atmosphere and interacts after crossing a column density  $X_0$ . The exponential distribution of  $X_0$  is determined by the interaction length  $\lambda_p(E_0)$ . It is a good approximation to neglect elastic and quasi-elastic (target nucleus fragmentation) processes and consider the “production cross section” for inelastic processes where new hadronic particles are produced.

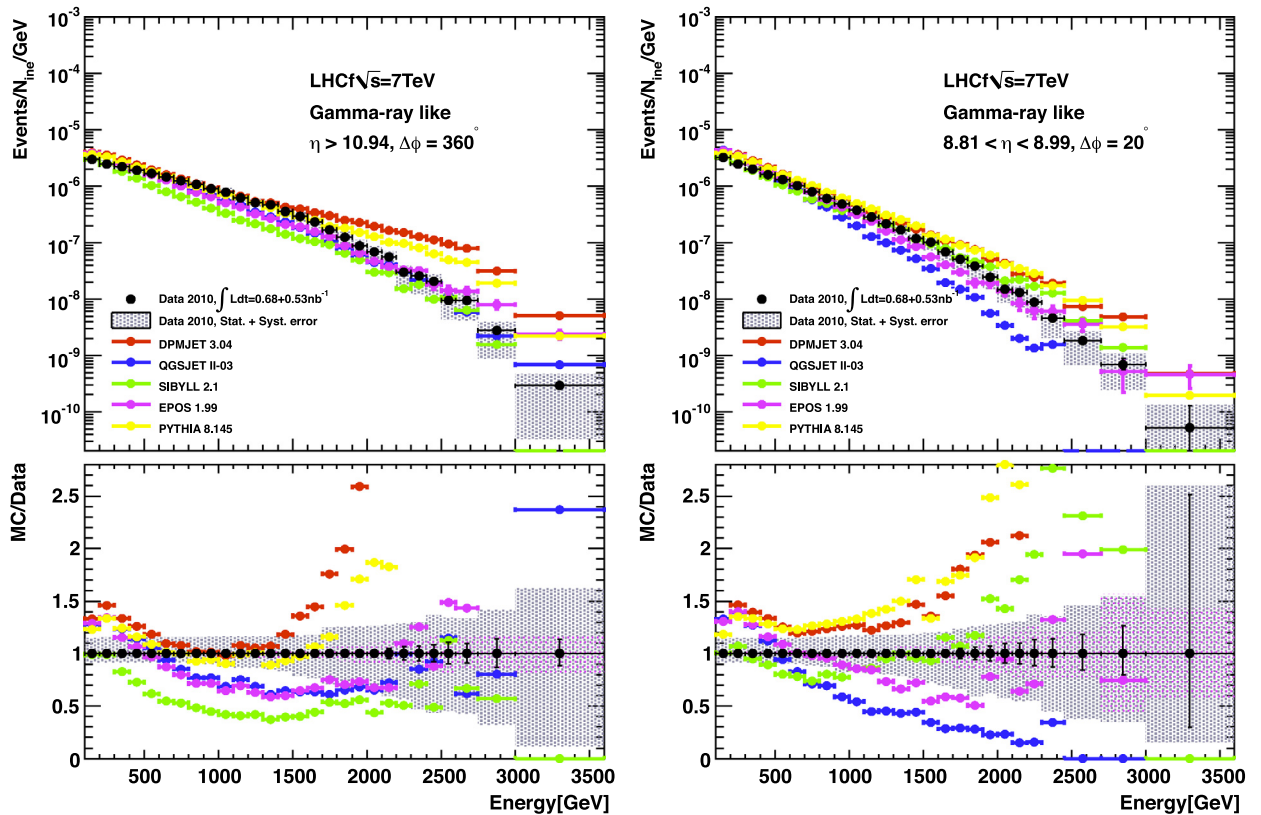


Fig. 4. Data of the LHCf detector at 7 TeV [11].

From the interaction point emerge several (at high energy many) particles and one needs to have a good description of how the energy and momentum carried by the primary proton is divided up among the final state particles. After the rapid decay of the hadronic resonances (such as  $\rho$ 's,  $\omega$ 's,  $\Delta$ 's and so on) the final state is composed by the hadrons that decay via electromagnetic or weak interactions. Essentially always, one high-energy baryon (the so-called "leading baryon") carries a large fraction of the primary energy. A precise description of the energy spectrum of this particle is of particular importance for the shower development. The final state contains also other low-energy nucleons to conserve the baryon number in the interactions, including the fragments of the target nucleus and possibly baryon/anti-baryon pairs created in the interaction. The most abundant secondaries are pions of the three charges, Kaon mesons (that contain a strange (anti-)quark) also account for a significant fraction (of the order of 10%) of the final state energy. Also the production of other mesons such as  $\eta$ 's is not negligible. The production of mesons (or baryons) that contain heavy ( $c$  and  $b$ ) quarks is suppressed dynamically, but for some observables (for example high-energy muon and neutrino production) it can also be an important problem.

The neutral pions decay rapidly into pairs of gamma rays ( $\pi^0 \rightarrow \gamma\gamma$ ), and additional photons are generated in the decay of  $\eta$  and  $\eta'$  mesons. These photons are the source of an electromagnetic shower that constitutes the largest component of the shower. See Fig. 4.

Stable particles, such as protons (and neutrons, that can be considered as stable for the time scale of shower development) propagate to a new interaction point where other particles are produced, and the process can be iterated until one reaches the ground level. In the case of long-lived particles that decay via the weak interaction (such as  $\pi^\pm$ , or kaons) one has to consider the competition between decay and interaction. The decay length of a particle grows linearly with momentum because of the Lorentz time dilatation ( $\ell_{\text{dec}} = c\tau p/m$ ), while the interaction length decreases slowly (approximately logarithmically) with increasing energy. The result is that high- (low-)energy particles interact (decay). The weak decays (such as  $\pi^+ \rightarrow \mu^+ \nu_\mu$ ) are a source of muons and neutrinos that form two other fundamental components of a hadronic shower.

Showers generated by primary nuclei have a structure that is essentially identical to that of the proton-induced showers. In the case of nucleus-nucleus collisions, only a fraction of the projectile nucleons "participate" in the interactions, and the remaining "spectator" nucleons emerge from the collision as an ensemble of fragments that travel with approximately the same velocity. The modeling of the shower requires a calculation of the distribution of a number of participating nucleons in the interaction and of the properties of nuclear fragmentation (for more discussion see, for example, [23]).



Because of its complex structure, the simplest and most accurate method for the calculation of the development of cosmic ray showers is the use of a Monte Carlo code. Such a code has to contain several elements: the structure of the atmosphere; the electromagnetic processes that control the development of purely electromagnetic showers (bremsstrahlung and pair production) and the propagation of charged particles in matter (multiple scattering and ionization losses); the spectra of final particles in weak decays (with the relevant matrix elements); and finally a detailed description of the properties of hadronic interactions for which one has to use one of the available models.

The fundamental problem of CR observations is to determine the energy and identity of the primary particle using the data collected by different sensors that have detected the shower. To discuss quantitatively the significance of the theoretical uncertainties on the modeling of hadronic interactions for CR studies, it is necessary to consider concrete examples of the type of measurements that are (or have been) in use.

Many air shower experiments observe only the particles that reach the ground level, effectively measuring a single layer of the shower development. The particles created in the shower are distributed with approximate cylindrical symmetry (broken by geomagnetic field effects and fluctuation effects) around the shower axis. They are detected by an array of sensors spread on the ground with an appropriate density over a sufficiently large area. In most cases, the observatory reconstructs the electromagnetic component of the shower ( $e^\pm$  and  $\gamma$ 's) and the muon number at the detector level. If, in addition, the detector is capable of observing, close to the shower axis, the hadronic component of the shower, the quality of the measurement can be significantly improved. The distribution for the pair of observables  $\{N_e, N_\mu\}$  can then be mapped into a distribution for the quantities  $\{A, E_0\}$ , that is the mass and energy of the primary particle (the number of photons does not give additional information, because the spectra of photons and  $e^\pm$  are in "equilibrium" and with good approximation one can predict one from the other). This program requires to have in hand the probability  $p(N_e, N_\mu; A, E_0, \theta)$  that a primary particle of mass  $A$ , energy  $E_0$  and zenith angle  $\theta$  generate a shower reconstructed with electron and muon numbers  $N_e$  and  $N_\mu$ . Obviously, with increasing  $E_0$ , the electron and muon numbers increase, while a larger mass number  $A$  (for a fixed primary energy) results in a larger muon number.

The program outlined above clearly depends on the model of hadronic interaction code used for estimating the response function  $p(N_e, N_\mu; A, E_0, \theta)$ , and the spectra obtained by experiments like Tibet III, Cascade and Cascade-Grande are given with 'labels', that indicate the Monte Carlo codes used for the shower simulation.

The task of reconstructing the energy in a shower has been much simplified, and the systematic error in the energy determination has been much reduced after the introduction by the Fly's Eye experiment of the technique of fluorescence light detection. The light emitted by the excitation of nitrogen molecules by charged particles in the shower can be detected to estimate the longitudinal profile of a shower, that is the number of charged particles  $N(X)$  present at the atmospheric depth  $X$ . The energy that the shower dissipates in air as ionization can be calculated from the profile performing the integral:

$$E_{\text{ion}} = \langle |dE/dX| \rangle \int dX N(X) \quad (4)$$

The total energy of the primary particle is then obtained including corrections to take into account the missing energy transported by muons (that deposit their energy in the ground) and neutrinos:

$$E_0 \simeq E_{\text{ion}} + E_\mu + E_\nu \quad (5)$$

In this estimate, the model dependence enters only for the missing energy correction, which is relatively small (approximately 20% for iron or 10% for protons at  $10^{18}$  eV, and 12% for iron or 6% for protons at  $10^{20}$  eV).

In hybrid experiments such as the Auger and Telescope Array observatories, the fluorescence method is used to calibrate the measurement of a surface array, that can achieve larger exposures, since the fluorescence light detection is only possible during dark (moonless) and clear (cloudless) nights.

The introduction of the fluorescence light method has allowed one to obtain a reasonably precise measurement of the energy spectrum of UHECR that is essentially independent of the assumptions on the nature of the primary particle and the modeling of hadronic interactions. However, one remains with the question of measuring the composition of the incoming particles.

As indicated in Eq. (4), the *area* under the curve of the longitudinal development  $N(X; E_0, A)$  of a primary of energy  $E_0$  and mass  $A$  is determined (to a good approximation) by the primary energy  $E_0$ , independently of  $A$ . On the other hand, the distribution  $N(X; E_0, A)$  does give information about the mass of the primary particle. For example, it is intuitive that the showers generated by a heavy nucleus are less penetrating than the showers generated by protons of the same total energy, but one has to take into account the fact that the shape  $N(X; E_0, A)$  also depends on the properties of hadronic interactions. It is also intuitively clear that if the cross section for hadronic interactions increases (the interaction length decreases) or if the spectra of secondary particles generated in the interactions are softer, the showers of a primary of a given mass and energy develop faster. The program to determine the composition of the UHECR from the shape of the longitudinal development is therefore critically dependent on the modeling of hadronic interactions.

The simplest way to characterize the shape of the longitudinal profile  $N(X)$  of a shower is to estimate the depth  $X_{\text{max}}$  where the shower size has its maximum. The distribution of  $X_{\text{max}}$  for showers with a certain energy  $E_0$  can be studied to obtain information about the mass composition of the particles. In particular, the average  $\langle X_{\text{max}}(E_0) \rangle$  can be interpreted

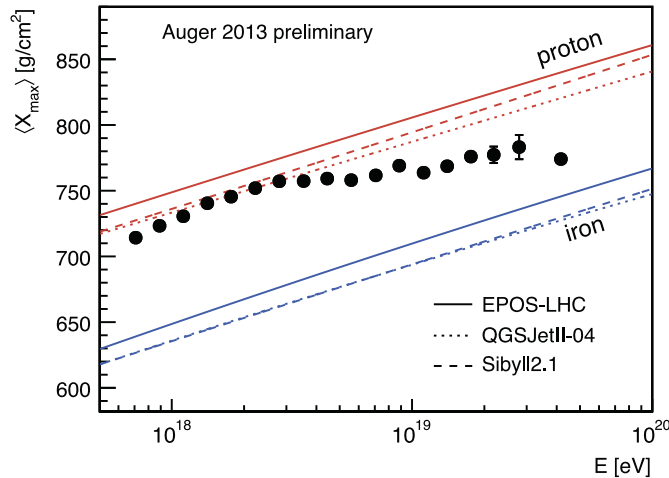


Fig. 5. Average  $X_{\max}$  measured by the Auger experiment [24] compared with air shower simulations using different hadronic interaction models.

as a measurement of the average mass of CR particles at the energy  $E_0$ . This idea is illustrated in Fig. 5, which shows the measurements of  $\langle X_{\max}(E_0) \rangle$  obtained by the Auger observatory [24] and compares them with calculations performed using different Monte Carlo codes [17–20] for showers generated by protons and iron nuclei.

For a purely electromagnetic shower (generated by an  $e^\pm$  or photon) the position of the shower maximum grows logarithmically with the primary particle energy, with a slope equal to the radiation length in air  $\lambda_0$ :

$$\langle X_{\max}(E_0; \gamma) \rangle = \lambda_0 \ln(E_0/\varepsilon) \quad (6)$$

(where  $\varepsilon$  is the critical electron energy in the air). An analytic derivation of this result is given for example in Rossi and Greisen [27]. The logarithmic dependence on the energy can be understood qualitatively as the consequence of the fact that an energy-independent radiation length determines the interaction points for the two processes (bremsstrahlung and pair production) that generate the shower, and in both cases the energy of a particle is “split” in an energy-scale independent way. These arguments are illustrated pedagogically in the well-known toy model introduced by Heitler [28], where the shower is formed by a single (electron/photon) particle type that after a “splitting length”  $\lambda$  divides into two particles, each with one half the energy, until the critical energy  $\varepsilon$  is reached. The shower develops to the maximum size  $N_{\max} = E_0/\varepsilon$  at the depth  $X_{\max} = \lambda \log_2(E/\varepsilon)$ .

Inspecting Fig. 5, one can see that also in the case of hadronic showers, for a constant mass  $A$  of the primary particle, the calculated  $\langle X_{\max}(E_0, A) \rangle$  grows approximately logarithmically with energy:

$$\langle X_{\max}(E_0, A) \rangle \simeq X_A + D \ln E_0 \quad (7)$$

with an “elongation rate”  $D$  that varies only slowly with energy. This result can be understood as a generalization of the arguments developed above for electromagnetic showers. In the case of hadronic showers, one must take into account the facts that when the energy of the interacting particle grows, its interaction length becomes shorter, and the particles in the final state increase in multiplicity and become progressively softer. Because of these effects, the average  $X_{\max}$  grows approximately logarithmically with energy, but with a slope (or elongation rate) that is smaller than what is found for electromagnetic showers. The slope is also not exactly independent of energy, and its precise value depends on the properties of hadronic interactions.

The average  $X_{\max}$  of the showers generated by a primary of energy  $E$  and mass  $A$  is approximately equal to the  $\langle X_{\max} \rangle$  of a proton shower of energy  $E/A$ . Using Eq. (7), this implies:

$$\langle X_{\max}(E_0, A) \rangle \simeq \langle X_{\max}(E_0, p) \rangle - D \ln A \quad (8)$$

Different primaries are characterized by roughly parallel lines in the  $\{\langle X_{\max} \rangle, \log E\}$  plane.

Combining Eqs. (7) and (8), the functions  $\langle X_{\max}(E_0, A) \rangle$  are, for a limited range of energy, reasonably well determined by two parameters, the value  $\langle X_p(E_0) \rangle$  at one energy and the elongation rate  $D$ . It is then easy to see how the measurement of  $\langle X_{\max}(E) \rangle$  can be mapped into an estimate of  $\langle \ln A(E) \rangle$ .

The program outlined above is of course limited by uncertainties in the modeling of the hadronic interactions that determine the two parameters  $\langle X_p(E_0) \rangle$  and  $D$ . Inspecting Fig. 5, one can conclude that the average mass of the cosmic rays becomes heavier with increasing energy, but for example the composition at  $E_0 \simeq 2 \times 10^{18}$  eV is pure protons for the models QGSJET, but contains a significant amount of nuclei using the model EPOS. The main difference between the models shown in Fig. 5 is associated with progressively stronger softening of the inclusive spectra going from EPOS (the most penetrating showers) to QGSJET (least penetrating showers).



The same experimental study on  $\langle X_{\max}(E) \rangle$  has been performed by the HiRes and Telescope Array detectors [25,26]. The data of the different experiments are not in good agreement, as neither TA nor HiRes see the average mass becoming heavier at the highest energies. In fact, HiRes concludes that the CR is dominated by protons above  $E \simeq 2 \times 10^{18}$  eV. As of today, a consistent interpretation of all the data is not yet possible.

Some natural and important questions emerge immediately. Which model represents best our current understanding of hadronic interaction? The spread of the predictions of the available models is often taken as an estimate of the systematic error associated with the theoretical uncertainties on hadronic interactions (using implicitly the assumptions that all models are of reasonably good quality). Is this a reasonable estimate? It is also, at least logically, possible, that all models are incorrect, and that some new unexpected phenomena become important at high energy. One should also remember that all the models in use for CR simulations attempt to describe the same experimental data and share a number of common assumptions (or perhaps prejudices). If the data have systematic errors, or some assumptions are flawed, this could lead to incorrect (and similar) predictions for all models.

The methodology outlined above (where one first constructs a model for hadronic interactions and then uses the model to determine the CR composition) could perhaps also be reversed. There are in fact methods to estimate the composition of cosmic rays, that are completely independent of the modeling of hadronic interactions. One such method uses the Milky Way as a magnetic spectrometer, measuring the deviation of particles generated by known sources. Having a sufficient precise knowledge of the galactic field, one can calculate the electric charge of the particles (the momentum is measured experimentally). In principle, it could also be possible to interpret features in the CR spectrum as the imprints on a smooth injection spectrum of energy losses that depend on the nature of the primary particles. Examples of these effects are the GZK suppression due to pion photoproduction by protons, the thresholds for photodisintegration of different nuclei or the ‘dip’ associated with the threshold for  $e^+e^-$  pair production. More speculatively it could be possible in the future to estimate the CR composition from multi-messenger (photon and neutrino) observations of the sources. Using these astrophysical methods to estimate the CR composition, it would become possible to interpret the observed properties of shower development to obtain information about hadronic interactions.

As an illustration, if one assumes that most of the UHECR particles are protons (as advocated in some astrophysical scenarios), the current Auger data on  $\langle X_{\max}(E) \rangle$  imply that the showers are much less penetrating than the current predictions. This in turn would imply that the inelastic cross sections are larger, and/or that the inclusive spectra in the final state are softer than the expectations.

More in general, one can hope (but in fact also realistically expect) that in the future it will be possible to determine simultaneously the composition of UHECR and the relevant properties of hadronic interactions. The key here is the consistency of different measurements of shower development. One very interesting example of this possibility is the recent measurement of the proton interaction length in the air obtained by the Auger Collaboration [29] for the observations of CR with energy  $E_0 \simeq 10^{18.24}$  eV ( $\sqrt{s} \simeq 57$  TeV for nucleon–nucleon interactions). The result:  $\sigma = 505 \pm 23(\text{stat}) -_{36}^{+28}(\text{sys})$  mb for the “production” cross section, on an average air nucleus is obtained with only limited assumptions about the cosmic ray composition at the energy considered (the He fraction is assumed to be below 25%). The result can be translated in the estimate for  $\sigma_{\text{tot}}^{pp}$  shown in Fig. 1.

#### 4. Conclusions

It is remarkable that the study of very-high-energy cosmic rays explores the dynamics of astrophysical accelerators with a size that is probably measured in light years (or more), but is also intimately related to the dynamics of hadronic interactions that operate at a length scale smaller than a fermi ( $10^{-13}$  cm). This can be seen as a striking example of the unity of physics.

The data collected at the high energy colliders, in particular at the LHC have been very important to test and improve our understanding of hadronic interactions, but many questions remain open, and result in uncertainties for the interpretation of CR observations. More efforts in the direction of new and better measurements on hadron collisions at accelerators are very desirable and should be strongly supported by the community interested in CR science.

Cosmic rays allow us to reach c.m. energies much higher than what is attainable with accelerators, and it is also, at least in principle, possible that valuable information about hadronic physics will be obtained using CR observations. The histories of cosmic ray physics and particle physics have been intimately related, and in many occasions, especially before the development of accelerators, new particles and new fundamental phenomena have been discovered in cosmic rays. One can expect that also in the future information will flow in both directions: from particle physics to astrophysics, and from astrophysics to particle physics.

#### References

- [1] K. Nakamura, et al., Particle Data Group Collaboration, J. Phys. G 37 (2010) 075021.
- [2] J. Beringer, et al., Particle Data Group Collaboration, Phys. Rev. D 86 (2012) 010001.
- [3] M.M. Block, F. Halzen, Phys. Rev. D 70 (2004) 091901, arXiv:hep-ph/0405174.
- [4] L.V. Gribov, E.M. Levin, M.G. Ryskin, Phys. Rep. 100 (1983) 1.
- [5] V. Barone, E. Predazzi, High Energy Particle Diffraction, Springer-Verlag, Berlin, 2002.
- [6] P. Lipari, M. Lusignoli, Phys. Rev. D 80 (2009) 074014, arXiv:0908.0495 [hep-ph].

- [7] P. Lipari, M. Lusignoli, Eur. Phys. J. C 73 (2013) 2630, arXiv:1305.7216 [hep-ph].
- [8] R.P. Feynman, Phys. Rev. Lett. 23 (1969) 1415.
- [9] R.D. Field, R.P. Feynman, Nucl. Phys. B 136 (1978) 1.
- [10] B. Andersson, G. Gustafson, G. Ingelman, T. Sjostrand, Phys. Rep. 97 (1983) 31.
- [11] O. Adriani, et al., Phys. Lett. B 703 (2011) 128, arXiv:1104.5294 [hep-ex].
- [12] T. Sjostrand, L. Lonnblad, S. Mrenna, arXiv:hep-ph/0108264.
- [13] T. Sjostrand, M. van Zijl, Phys. Rev. D 36 (1987) 2019.
- [14] T. Sjostrand, S. Mrenna, P.Z. Skands, Comput. Phys. Commun. 178 (2008) 852, arXiv:0710.3820 [hep-ph].
- [15] M. Bahr, S. Gieseke, M.H. Seymour, J. High Energy Phys. 0807 (2008) 076, arXiv:0803.3633 [hep-ph].
- [16] T. Gleisberg, et al., J. High Energy Phys. 0902 (2009) 007, arXiv:0811.4622 [hep-ph].
- [17] N.N. Kalmykov, S.S. Ostapchenko, Phys. At. Nucl. 56 (1993) 346;  
N.N. Kalmykov, S.S. Ostapchenko, Yad. Fiz. 56 (3) (1993) 105.
- [18] S. Ostapchenko, Phys. Rev. D 74 (2006) 014026, arXiv:hep-ph/0505259.
- [19] E.J. Ahn, R. Engel, T.K. Gaisser, P. Lipari, T. Stanev, Phys. Rev. D 80 (2009) 094003, arXiv:0906.4113 [hep-ph].
- [20] K. Werner, F.-M. Liu, T. Pierog, Phys. Rev. C 74 (2006) 044902, arXiv:hep-ph/0506232.
- [21] B. Alessandro, et al., arXiv:1101.1852 [hep-ex].
- [22] D. d'Enterria, et al., Astropart. Phys. 35 (2011) 98, arXiv:1101.5596 [astro-ph.HE].
- [23] J. Engel, T.K. Gaisser, T. Stanev, P. Lipari, Phys. Rev. D 46 (1992) 5013.
- [24] A. Letessier-Selvon, Pierre Auger Collaboration, in: 33rd ICRC, 2013, arXiv:1310.4620 [astro-ph.HE].
- [25] R.U. Abbasi, et al., HiRes Collaboration, Phys. Rev. Lett. 104 (2010) 161101, arXiv:0910.4184 [astro-ph.HE].
- [26] P. Sokolsky, TA Collaboration, HiRes Collaboration, EPJ Web Conf. 52 (2013) 06002.
- [27] Bruno Rossi, Kenneth Greisen, Rev. Mod. Phys. 13 (1941) 240.
- [28] W. Heitler, International Series of Monographs on Physics, Clarendon Press, Oxford, UK, 1954.
- [29] P. Abreu, et al., Pierre Auger Collaboration, Phys. Rev. Lett. 109 (2012) 062002, arXiv:1208.1520 [hep-ex].